Matrices of Physiologic Stiffness Potently Inactivate Idiopathic Pulmonary Fibrosis Fibroblasts

Aleksandar Marinković[1], Fei Liu[1], and Daniel J. Tschumperlin[1]

[1]Division of Molecular and Integrative Physiological Sciences, Department of Environmental Health, Harvard School of Public Health, Boston, Massachusetts

Fibroblasts from patients with idiopathic pulmonary fibrosis (IPF) have been shown to differ from normal lung fibroblasts in functional behaviors that contribute to the pathogenesis of IPF, including the expression of contractile proteins and proliferation, but how such behaviors vary in matrices with stiffness matched to normal and fibrotic lung tissue remains unknown. Here, we tested whether pathologic changes in matrix stiffness control IPF and normal lung tissue–derived fibroblast functions, and compared the relative efficacy of mechanical cues to an antifibrotic lipid mediator, prostaglandin E_2 (PGE_2). Fibroblasts were grown on collagen I–coated glass or hydrogel substrates of discrete stiffnesses, spanning the range of normal and fibrotic lung tissue. Traction microscopy was used to quantify contractile function. The CyQuant Cell Proliferation Assay (Invitrogen, Carlsbad, CA) was used to assess changes in cell number, and PGE_2 concentrations were measured by ELISA. We confirmed differences in proliferation and PGE_2 synthesis between IPF and normal tissue–derived fibroblasts on rigid substrates. However, IPF fibroblasts remained highly responsive to changes in matrix stiffness, and both proliferative and contractile differences between IPF and normal fibroblasts were ablated on physiologically soft matrices. We also confirmed the relative resistance of IPF fibroblasts to PGE_2, while demonstrating that decreases in matrix stiffness and the inhibition of Rho kinase both potently attenuate contractile function in IPF-derived fibroblasts. We conclude that pathologic changes in the mechanical environment control important IPF fibroblast functions. Understanding how mechanical cues control fibroblast function may offer new opportunities for targeting these cells, even when they are resistant to antifibrotic pharmacological agents or biological mediators.

Keywords: pulmonary fibrosis; lung; extracellular matrix; fibroblast contractility

CLINICAL RELEVANCE

Microscale changes in matrix stiffness accompany the development of lung fibrosis, and matrix stiffness itself can control important aspects of cell function that contribute to fibrogenesis. However, it remains unknown whether fibroblasts from patients with idiopathic pulmonary fibrosis (IPF) remain responsive to matrix stiffness, or have established an activated state that is independent of mechanical cues. We used synthetic matrices of defined stiffness to show that IPF-derived lung fibroblasts remain responsive to a pathologically relevant range of matrix stiffness. Although IPF fibroblasts show reduced responsiveness to the antifibrotic lipid mediator prostaglandin E_2, they retain equal or greater responsiveness to decreases in matrix stiffness and the inhibition of the stiffness-sensitive Rho kinase pathway, indicating that mechanical cues may offer unique and potent targets for inactivating IPF fibroblasts.

Idiopathic pulmonary fibrosis (IPF) is a devastating, progressive fibrosing disease with no proven pharmacological therapy (1). The fibroblast is the end effector cell of fibrosis, and fibroblasts increase in number and activation status during IPF. Scattered aggregates of proliferating fibroblasts are consistently observed in fibrotic lungs (2, 3), and the progression of IPF is accompanied by an excessive activation of lung fibroblasts to a synthetic and contractile myofibroblast phenotype responsible for the deposition, contraction, and remodeling of the lung's extracellular matrix (ECM) (4, 5).

To understand the pathogenic mechanisms at work in IPF, much effort has been devoted to identifying functional differences in IPF-derived fibroblasts compared with fibroblasts isolated from normal lung tissue. These efforts have demonstrated, among a host of changes, that IPF fibroblasts are more contractile (6), express higher concentrations of α–smooth muscle actin (α-SMA) (7, 8), Type I collagen (8–10), and tissue inhibitors of metalloproteinase (11) than do normal lung tissue–derived fibroblasts, and are characterized by pathologic integrin signaling (12) and an invasive phenotype (13). Relative to normal cells, IPF-derived fibroblasts have also been shown to express lower concentrations of cyclooxygenase-2 (COX-2), produce less of the antifibrotic lipid mediator prostaglandin E_2 (PGE_2) (14, 15), and exhibit resistance to this antifibrotic lipid mediator applied exogenously (16). These findings suggest that fibroblasts within fibrotic tissues fundamentally differ from the normal fibroblast population of the lung, contributing to both the pathogenesis of fibrosis and resistance to treatment.

Recently, the lung ECM was shown to stiffen significantly during fibrosis (17), and transitions in matrix stiffness across the pathologically relevant range have evoked many of the same functional changes in fibroblast biology seen in IPF-derived fibroblasts, including the enhanced tension-generating myofibroblastic differentiation of fibroblastic cells (18–20), as well as increased proliferation, apoptosis resistance, and collagen synthesis (17). In addition, the combination of stiff mechanical environment and increasing fibroblast contractility has been shown to promote the activation of transforming growth factor-β, whereas compliant matrices attenuate such activation (19). The differences between IPF and normal fibroblasts were largely identified through the study of cells on substrates that were either rigid or poorly defined mechanically, leaving open

(*Received in original form August 27, 2012 and in final form October 29, 2012*)

This work was supported by National Institutes of Health grants RO1HL092961 (D.J.T.) and T32HL007118 (A.M.).

Author Contributions: A.M. and D.J.T. conceived and designed the research. A.M. and F.L. performed the experiments. A.M. and D.J.T. analyzed the data. A.M. prepared the figures and drafted the manuscript. A.M., F.L., and D.J.T. edited and approved the final version of the manuscript.

Correspondence and requests for reprints should be addressed to Daniel J. Tschumperlin, Ph.D., Molecular and Integrative Physiological Sciences, Department of Environmental Health, Harvard School of Public Health, 665 Huntington Ave., SPH1-309, Boston, MA 02115. E-mail: dtschump@hsph.harvard.edu

This article has an online supplement, which is accessible from this issue's table of contents at www.atsjournals.org

Am J Respir Cell Mol Biol Vol 48, Iss. 4, pp 422–430, Apr 2013

Originally Published in Press as DOI: 10.1165/rcmb.2012-0335OC on December 20, 2012
Internet address: www.atsjournals.org

the questions of whether IPF-derived fibroblasts remain responsive to the stiffness of their mechanical environment, and whether differences in IPF and normal tissue–derived fibroblasts are dependent on pathologically stiff environments.

Here, we designed experiments to determine whether IPF and normal tissue–derived fibroblasts differ in their responses to a pathophysiological range of matrix stiffnesses, focusing on contractility and cell proliferation, as well as on the synthesis of PGE_2 and cell responsiveness to exogenous PGE_2. Based on previous observations that matrix stiffening promotes increased Rho kinase (ROCK) activity (21), we also compared the responses of IPF and normal fibroblasts to a ROCK inhibitor (Y-27632). Our results demonstrate that IPF fibroblast contractile function and proliferation are highly responsive to changes in matrix stiffness, and that differences in IPF and normal fibroblasts seen on rigid matrices are ablated on physiologically soft matrices. Moreover, IPF fibroblasts that are resistant to the PGE_2-mediated inhibition of contractile function remain highly responsive to decreases in matrix stiffness and the inhibition of stiffness-sensitive Rho kinase. Based on these observations, we conclude that pathologic changes in the mechanical environment are important contributors to IPF fibroblast function, and that fibroblast responses to mechanical cues may offer unique and potent targets for inactivating IPF fibroblasts.

MATERIALS AND METHODS

Cell Culture

Fibroblasts isolated from the lungs of five subjects diagnosed with IPF and four normal subjects were kindly provided by Dr. Carol Feghali-Bostwick (University of Pittsburgh, Pittsburgh, PA). Fibroblasts were either cultured from the explanted lungs of patients with IPF who underwent lung transplantation at the University of Pittsburgh Medical Center, under a protocol approved by the University of Pittsburgh Institutional Review Board, or from normal lung tissue obtained from organ donors. Approximately 2-cm^3 pieces of peripheral lung from which the pleural margin was removed were minced, and fibroblasts were cultured as previously described (22). Cells were then cultured in Dulbecco's Modified Eagle's Medium containing 4.5 g/L glucose, L-glutamine, and sodium pyruvate, and supplemented with 10% FBS, 100 U/ml penicillin, and 100 μg/ml streptomycin (all from Mediatech, Manassas, VA) in a humidified incubator with an atmosphere containing 5% CO_2 at 37°C. For the experiments that will be described, cells were used at passages 3–5.

Compliant Matrices and Cell Number Assays

Fibroblasts were seeded at 25 cells/mm^2 on glass or polyacrylamide (PA) hydrogel substrates of one of three discrete elastic (Young's) moduli (1, 6, and 20 kPa), cast in multiwell plates. All surfaces were functionalized with a surface coating of 10 μg/ml of collagen I, as previously described (23). Four hours after seeding, the initial cell number was assessed by a CyQuant NF Cell Proliferation Assay (Invitrogen, Carlsbad, CA), and the indicated concentrations of PGE_2 or Y-27632 or vehicle controls were added to remaining wells. Seventy-two hours later, the CyQuant assay was used again to determine the cell number in each well.

Traction Assays

We used improved-throughput traction microscopy (20) to measure traction fields generated on polyacrylamide gel surface by individual fibroblasts, and computed root–mean–square tractions (RMSTs) to compare the obtained traction fields, under both control and the indicated treatment conditions. In this assay, 24 hours before traction measurements, cells were seeded at 10 cells/mm^2 in 24-well plates containing PA gel substrates of one of three discrete elastic moduli (1, 6, and 20 kPa). Hydrogel polymerization, gel surface derivatization, and the attachment of fluorescent, 0.2-μm-diameter, sulfate-modified latex microspheres (Invitrogen) were performed as described previously (20). After rinsing in distilled water, the gels were ultraviolet light–sterilized and functionalized by incubation for 2 hours with 10 μg/ml of sterile collagen I (PureCol; Advanced BioMatrix, San Diego, CA) in PBS. Cells were cultured on PA gels for 24 hours before baseline traction measurements. Wells were treated with indicated concentrations of PGE_2 or Y-27632 for 120 minutes, and traction measurements were repeated. For each cell, the RMST was calculated from estimated traction fields corresponding to measured surface-bound bead displacement fields, as described previously (20).

PGE_2 Assays

PGE_2 enzyme–linked immunosorbent assays were performed according to the manufacturer's instructions (Cayman Chemicals, Ann Arbor, MI) with the cell culture media collected from the wells, 72 hours after the fibroblasts were seeded.

Statistical Analysis

Statistical tests were performed using Excel (Microsoft, Redmont, WA) and Stata (StataCorp LP, College Station, TX). Additional detailed methods are available in the online supplement.

RESULTS

IPF-Derived Fibroblasts Exhibit Phenotypic Differences from Normal Fibroblasts, but Remain Highly Responsive to Matrix Stiffness

Guided by evidence that substrate mechanical properties prominently influence contractile force–generating capacity (18, 24), we tested whether fibroblasts derived from IPF and normal lungs exert different traction forces on matrices spanning an elastic modulus range observed in normal (1 kPa) and fibrotic (6 and 20 kPa) lung tissue (17). As with a previously studied human fibroblast cell line (20), both normal tissue and IPF-derived lung fibroblasts exhibited dramatic decreases in traction forces with decreasing matrix stiffness (Figure 1A). This behavior was uniformly observed in all five IPF-derived and all four normal lung tissue–derived primary fibroblast populations (Figure 1B), with significant decreases in tractions found in each donor line with decreasing matrix stiffness. When analyzed together, IPF fibroblasts exerted significantly higher tractions compared with their normal counterparts only when cultured on matrices with elastic moduli observed in fibrotic lung parenchyma (6 and 20 kPa) (17) (*$P < 0.05$, two-tailed t test; Figure 1C). Strikingly, on matrices with elastic moduli matched to the median of normal lung tissue (1 kPa) (17), traction magnitudes were indistinguishable between the two fibroblast populations (Figure 1C), effectively reverting the contractile IPF-derived fibroblast phenotype. The percent reduction in RMSTs between the fibrotic (20 kPa) and normal (1 kPa) stiffness condition was measured at 86% ± 2% in IPF, and 79% ± 4% in normal lung fibroblasts (mean ± SD, $P < 0.05$, two-tailed t test). Of note, the difference in traction-generating capacity between normal tissue–derived and IPF-derived fibroblasts seen on stiffer matrices was small compared with the effect of reducing matrix stiffness, suggesting a prominent role for matrix stiffness in driving this cellular phenotype.

To evaluate a second stiffness-dependent aspect of fibroblast biology relevant to fibrosis, we measured the changes in cell numbers of both IPF and normal lung tissue–derived fibroblasts across the same range of matrix stiffness. Within each donor line, we observed consistent trends toward lower cell numbers with decreasing matrix stiffness (Figure 2A), with the exception of IPF-14, which exhibited little dependence on matrix stiffness. When analyzed together, both IPF and normal fibroblast cell

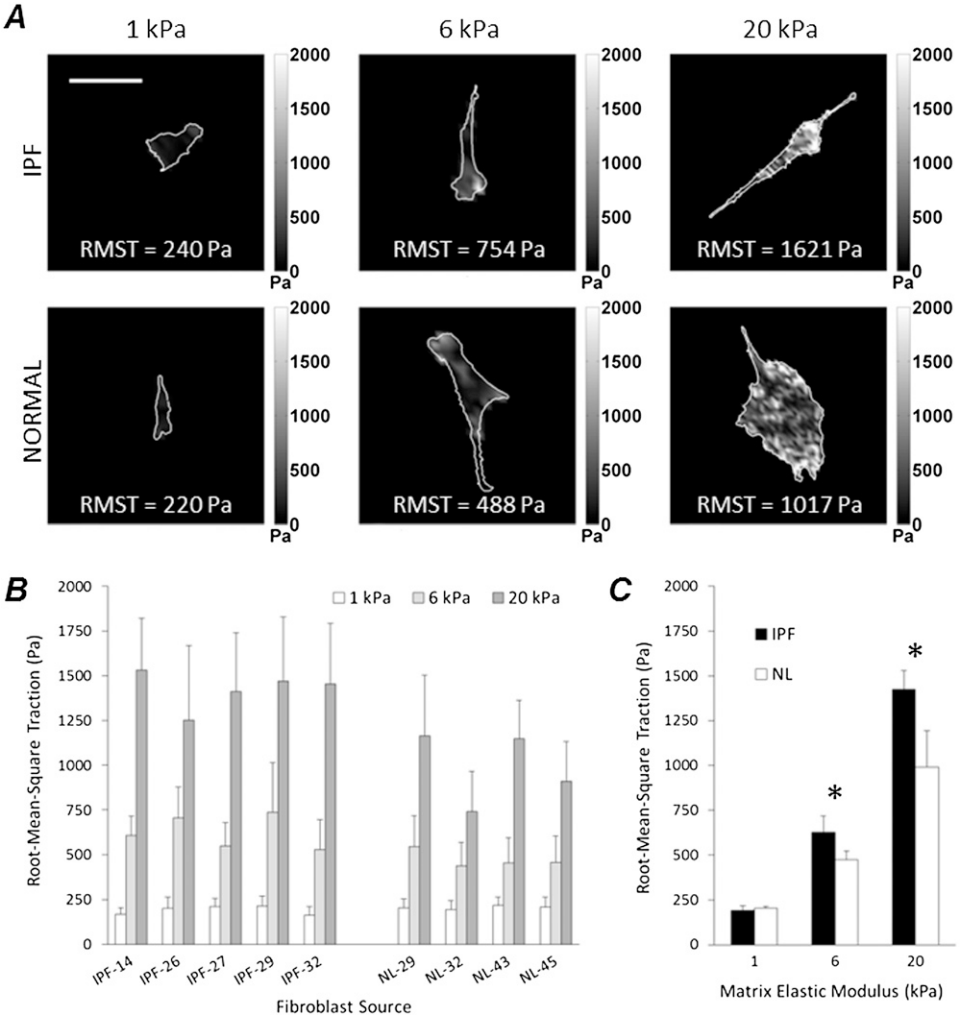

Figure 1. Matrix stiffness controls traction generation in idiopathic pulmonary fibrosis (IPF) fibroblasts and normal lung fibroblasts. (*A*) Representative maps of traction fields from IPF (*upper row*) and normal (*lower row*) fibroblasts were obtained in polyacrylamide gel substrates with elastic moduli of 1, 6, and 20 kPa, as indicated in each image. Grayscale traction magnitudes (in Pa) are shown next to the maps. Root–mean–square tractions (RMSTs) were calculated for each traction field, and are shown on the maps as RMST values. *Scale bar* = 100 μm. (*B*) RMSTs were computed from the traction fields of primary human lung fibroblasts derived from fibrotic (IPF) or normal (NL) lung tissue and grown on substrates resembling normal (1 kPa, *white*), or fibrotic (6 kPa, *light gray*; 20 kPa, *dark gray*) stiffness matrices. Increasing matrix stiffness promoted the generation of traction, regardless of cell source. Data represent the mean ± SD from 15 cells per source per stiffness condition. (*C*) RMSTs were averaged across disease state for each matrix-stiffness condition, from the data presented in *B*. *Asterisks* mark statistically significant differences in RMSTs between IPF and normal cells under the indicated matrix-stiffness conditions (*$P < 0.05$, two-tailed *t* test). Data represent the mean ± SD.

numbers were attenuated by reductions in matrix stiffness relative to the rigid glass condition ($P < 0.05$, two-tailed z-test for significant difference in cell accumulation rate relative to glass, under each stiffness condition), with the exception of IPF fibroblasts cultured on 20 kPa PA gel substrates (P value = 0.37, Figure 2B). When comparing IPF and normal lung fibroblasts, we documented significantly higher cell numbers accumulating in normal tissue–derived fibroblasts relative to IPF-derived fibroblasts, but only on rigid glass matrices (*$P < 0.05$, two-tailed *t* test, Figure 2B). As was the case with cell tractions, reducing matrix stiffness to physiologically soft conditions reverted the phenotypic difference in proliferation rate, such that cell numbers were indistinguishable between IPF and normal tissue–derived cells on 1-kPa matrices.

The production of PGE_2 is another reported difference between IPF and normal lung fibroblasts (14, 15), and was also shown to be matrix stiffness–dependent (17). Hence we measured PGE_2 concentrations in the supernatants of cultured IPF and normal fibroblast lines, and normalized these concentrations to cell number. In agreement with previous observations, IPF cells produced significantly lower concentrations of PGE_2 on glass than did normal fibroblasts. This difference was preserved under all matrix stiffness conditions (Figure 3A). However, both IPF and normal tissue–derived fibroblasts significantly increased PGE_2 concentrations when grown on matrices matched to median normal lung tissue stiffness (1 kPa; $P < 0.05$, two-tailed *t* test), with an 111% increase between glass and 1 kPa in normal fibroblasts, and a 109% increase in IPF-derived cells (Figure 3B). These results demonstrate that although IPF-derived fibroblasts are phenotypically impaired in PGE_2 production, they are stimulated to increase production under normal physiologic matrix stiffness conditions, and respond to pathological increases in matrix stiffness with a reduced production of PGE_2.

IPF Fibroblast Responses to Matrix Stiffness Are Greater than or Equal to Effects of PGE_2 Treatment

Based on the previously documented differences in normal and IPF-derived fibroblasts regarding the antifibrotic effects of prostanoid PGE_2 (16, 25), we tested whether this soluble factor suppresses traction generation and cell accumulation in both normal fibroblasts and those from patients with IPF across a pathophysiological range of matrix stiffnesses. We first studied the dose-dependent and time-dependent responses (Figures 4A and 4B) of one fibroblast line from each group, and observed a similar magnitude and kinetics of reductions in cellular traction on 6-kPa matrices. Based on this preliminary analysis, we chose a 5-μM PGE_2 concentration and 2-hour time point for all subsequent traction measurements (Figure 4C). When extending our analysis across all donors, both normal tissue–derived and IPF-derived fibroblasts responded to PGE_2 treatment with statistically significant declines in tractions across all donors and across all substrate stiffness conditions, with the exception of IPF-26 on 1 kPa, and IPF-32 on 1-kPa and 6-kPa gels (Figure 4C, #two-tailed z-test for significant change in RMST).

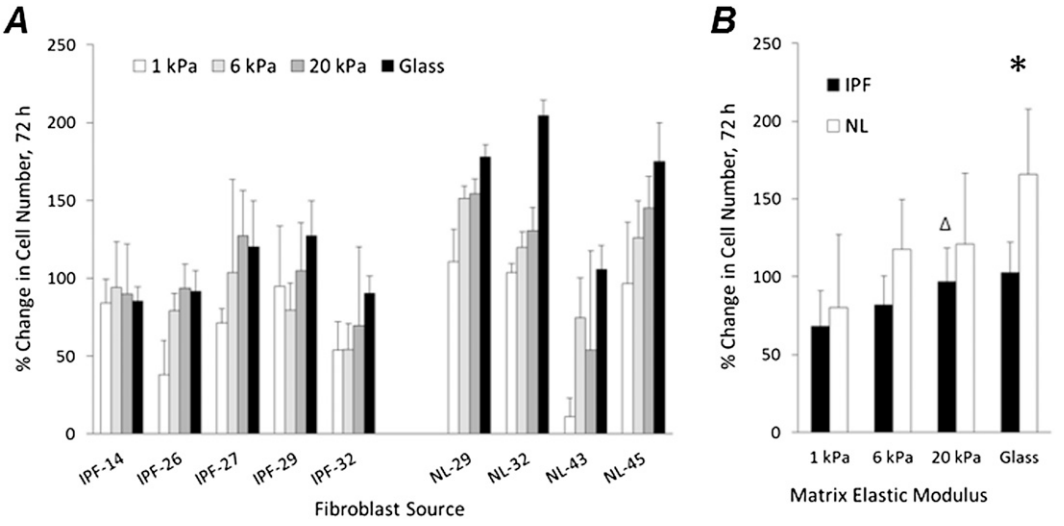

Figure 2. Matrix stiffness controls the proliferation of IPF and normal lung fibroblasts. (*A*) Percent changes in cell number over 72 hours after seeding. Fibroblasts derived from fibrotic (IPF) or normal (NL) lung tissue were initially seeded at a density of 25 cells/mm^2 on the polyacrylamide gels with elastic moduli of 1 kPa (*white*), 6 kPa (*light gray*), and 20 kPa (*dark gray*), or glass (*black*). Data represent the mean ± SD from three independent measurements for each cell source and stiffness condition. (*B*) Percent changes in cell number were averaged within the disease state for each stiffness condition, from the data presented in *A*. *Asterisks* are used to label either statistically significant differences in cell accumulation between IPF and normal fibroblasts on glass (*$P < 0.05$, two-tailed *t* test), or no significant difference in accumulation rates between IPF cells grown on 20-kPa polyacrylamide (PA) gels and glass ($^{\Delta}P = 0.37$, two-tailed *t* test). Data represent the mean ± SD.

Across the group of IPF fibroblasts, the average RMST dropped 17% ± 3% (mean ± SD), 20% ± 4%, and 28% ± 3% (Figure 4D) on 1-kPa, 6-kPa, and 20-kPa PA gel substrates, respectively (P value < 0.0001, two-tailed z-test, for all gel stiffness conditions) after PGE_2 treatment. In normal lung fibroblasts, the decline in average RMST was 27% ± 3%, 49% ± 5%, and 40% ± 3% (Figure 4D), on 1-kPa, 6-kPa, and 20-kPa PA gel substrates, respectively ($P < 0.0001$, two-tailed z-test, for all gel stiffness conditions). In aggregate, a significantly greater decline in average RMSTs was evident after PGE_2 treatment in normal versus IPF fibroblasts on 20-kPa gels (P value $= 0.024$, two-tailed t test) and 6-kPa gels ($P = 0.004$, two-tailed t test). This difference in PGE_2 responsiveness was attenuated on 1-kPa PA substrates, and narrowly failed to achieve statistical significance ($P = 0.057$, two-tailed t test).

One interesting comparison made possible by our study involved analyzing changes in traction after antifibrotic prostanoid treatment versus the differences in traction observed under different underlying matrix stiffness conditions. Interestingly, when we compared the effects of PGE_2 to the differences in traction observed between 6 and 1 kPa (i.e., a difference in stiffness roughly equivalent to the median modulus in fibrotic and normal lung tissue) (17), we found a clear segregation between IPF and normal tissue–derived fibroblasts. Normal fibroblasts exhibited similar reductions in traction in response to PGE_2 and alterations in matrix stiffness, whereas IPF fibroblasts were much less responsive to PGE_2 treatment, while retaining a similar response to matrix stiffness (Figure 4E). Moreover, the average drop in mean RMST found between 6 and 1 kPa was significantly higher in IPF than in normal fibroblast lines, namely, −69% ± 2% and −56% ± 2%, respectively ($P < 0.003$, two-tailed t test). These results demonstrate the potency of ECM stiffness within the range of fibrotic and normal lung elastic moduli in controlling fibroblast tractions, particularly in IPF cells that are relatively resistant to PGE_2 treatment.

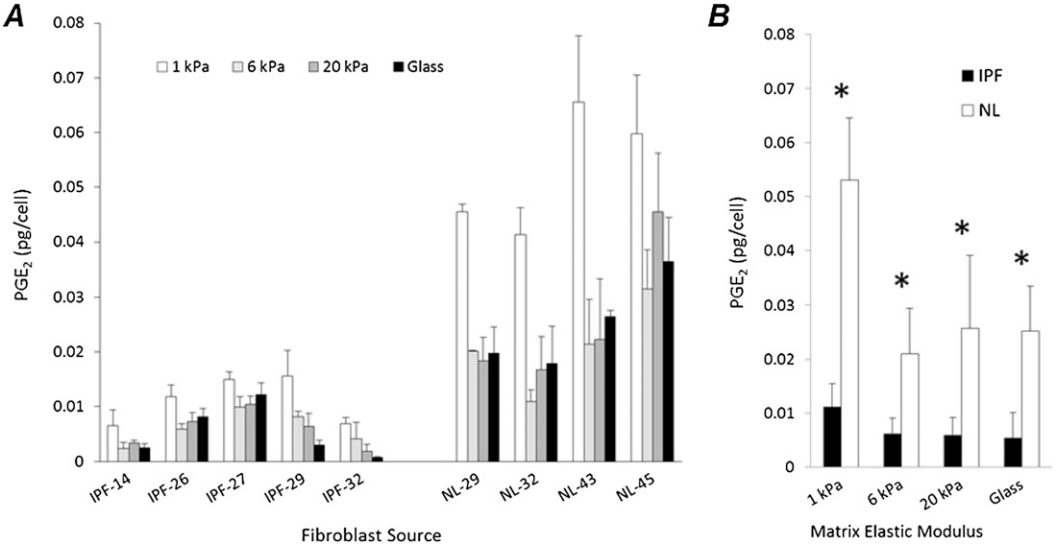

Figure 3. IPF fibroblasts exhibit diminished production of prostaglandin E_2 (PGE_2), but increased production on physiological stiffness matrices. (*A*) PGE_2 concentrations in IPF and normal fibroblast cell culture supernatants were normalized to corresponding cell numbers. Cells were grown for 72 hours on the PA gels with elastic moduli of 1 kPa (*white*), 6 kPa (*light gray*), and 20 kPa (*dark gray*), or glass (*black*). Data represent the mean ± SD from three independent measurements for each fibroblast source and stiffness condition. (*B*) PGE_2 concentrations were averaged across disease state for each matrix stiffness condition, from data presented in *A*. Under the indicated stiffness conditions, *asterisks* mark statistically significant differences in measured average PGE_2 concentrations between fibroblasts from normal and diseased lungs (*P value < 0.05, two-tailed t test). Data represent the mean ± SD.

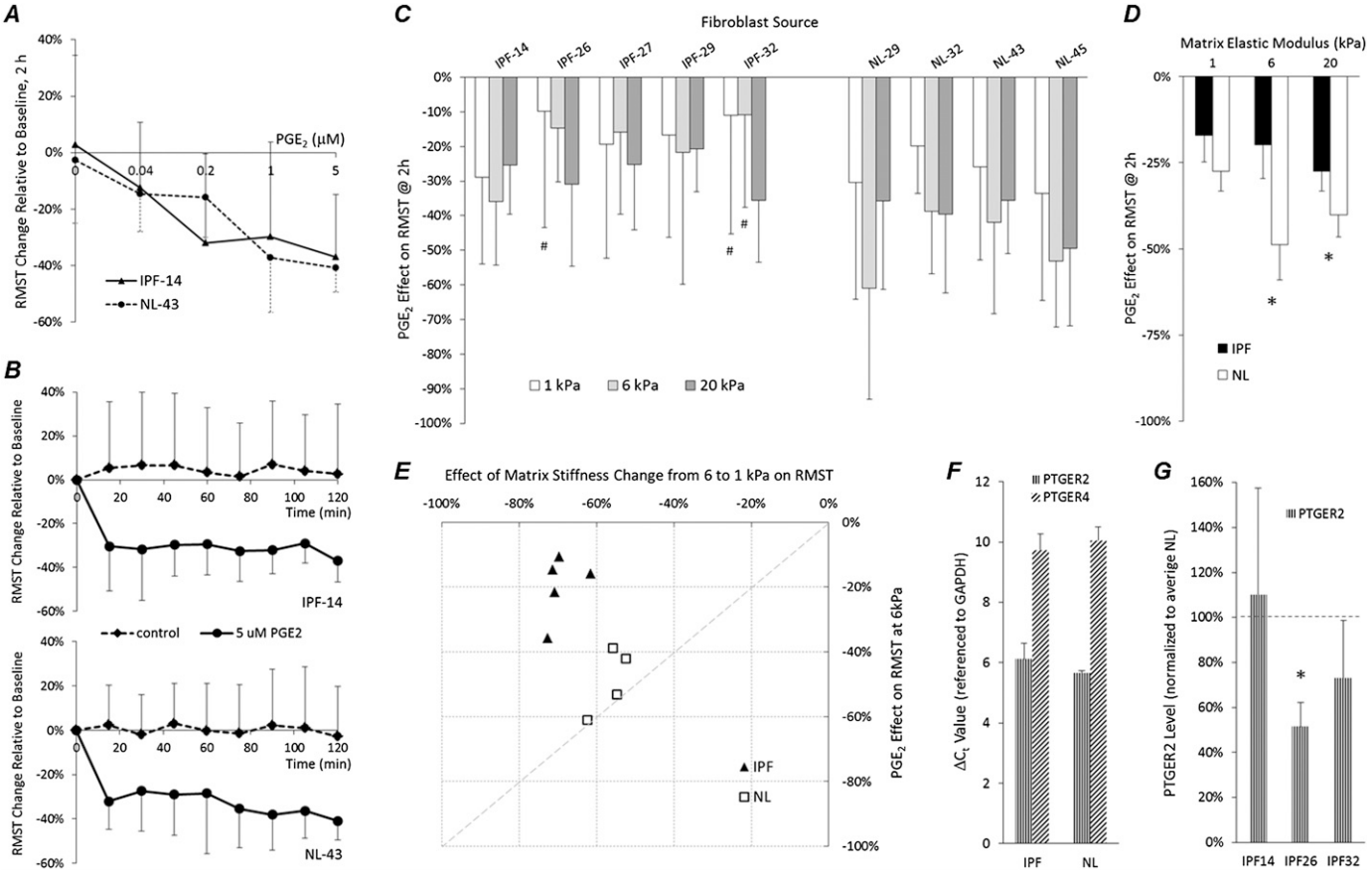

Figure 4. PGE_2 more potently attenuates the traction generation of normal compared with IPF fibroblasts on fibrotic stiffness matrices. (*A*) Two-hour PGE_2 dose–response effect on RMST changes, relative to time zero baseline for one fibrotic (IPF-14) and one normal (NL-43) fibroblast line grown on 6-kPa gels. Data represent the mean ± SD of 10 cells per dose for each fibroblast source. (*B*) Time course of average RMST changes from time zero baselines after the addition of 5 μM PGE_2 (*solid line*) and without treatment (*dashed line*), measured in one IPF (*top*) and one normal (*bottom*) fibroblast line grown on PA gels with elastic moduli of 6 kPa. For each time point, data represent the mean (± SD) RMST change obtained from 10 cells. (*C*) Drop in RMSTs is shown as the percent change from baseline for each cell, measured 2 hours after treatment with 5 μM PGE_2. Fibroblasts derived from fibrotic (IPF) or normal (NL) lungs were grown on PA gel substrates with elastic moduli of 1 kPa (*white*), 6 kPa (*light gray*), and 20 kPa (*dark gray*). #Two-tailed z-test for significant change in RMST. (*D*) Average RMST drop across disease state for each stiffness condition, from measurements shown in *B*. *Asterisks* are used to mark statistically significant difference in RMST drop between IPF and normal fibroblasts under indicated stiffness conditions ($P < 0.05$, two-tailed *t* test). Data represent the mean ± SD. (*E*) Scatterplot compares the effects on RMST of 5 μM PGE_2 and changes in substrate stiffness from 6 to 1 kPa. Data points indicate the average percent drop in RMST on 6-kPa gels, 2 hours after treatment with 5 μM PGE_2, versus percent difference in mean RMST on 6-kPa and 1-kPa gels for each fibroblast source (normal [NL] fibroblasts, *open squares*; IPF, *solid triangles*). (*F*) Difference in real-time PCR cycle threshold (ΔC_t) values of E prostanoid (EP) receptor genes PTGER2 (EP2) and PTGER4 (EP4), referenced to glyceraldehyde 3–phosphate dehydrogenase C_t values. Data represent the mean ± SD of three IPF and three normal fibroblast lines. (*G*) PTGER2 transcript levels in each IPF fibroblast line were normalized to average transcript levels in three normal lung fibroblast lines. *Asterisks* mark statistically significant differences in PTGER2 mRNA concentrations, compared with the average transcript level in normal fibroblast lines ($P < 0.05$, two-tailed z-test). Data represent the mean ± SD of two independent experiments.

To determine whether variations in the expression of prostanoid receptors could account for the observed differences in IPF and normal fibroblast PGE_2 responsiveness, we measured relative transcript abundance of E prostanoid (EP) receptor genes PTGER2 (EP2) and PTGER4 (EP4), the EP receptors responsible for the antifibrotic effects of PGE_2, in three representative IPF and normal fibroblast lines (PTGER1 and PTGER3 were not detectable by quantitative PCR; data not shown). We previously demonstrated that PTGER transcript levels are insensitive to matrix stiffness (17), and similar preliminary results were observed here (data not shown). Therefore we limited our analysis to cells grown on rigid matrices. Relative to the transcript levels of the housekeeping gene glyceraldehyde 3–phosphate dehydrogenase, PTGER4 transcript levels were approximately 16-fold lower than those of PTGER2 in both IPF and normal cells, consistent with the previously observed higher abundance of EP2 receptor expression (26) (Figure 4F). To analyze further variations in PTGER2 expression in IPF fibroblasts, we compared each IPF line to the average transcript levels in the three normal fibroblast lines (which were tightly clustered; Figure 4F). Similar to previous observations (16, 27), we noted highly variable reductions in PTGER2 expression in individual IPF fibroblast lines (Figure 4G) that were not systematically related to functional PGE_2 responses (Figure 4C).

We took a similar approach in analyzing cell numbers by examining the dose-dependent effects of PGE_2 on cell accumulation at 72 hours on matrices of intermediate substrate stiffness (6 kPa), using a single IPF and normal tissue–derived fibroblast line (Figure 5A). Based on this analysis, we used 1 μM PGE_2 and 72 hours of treatment for subsequent experiments. In agreement with previous findings (16), we observed a significant

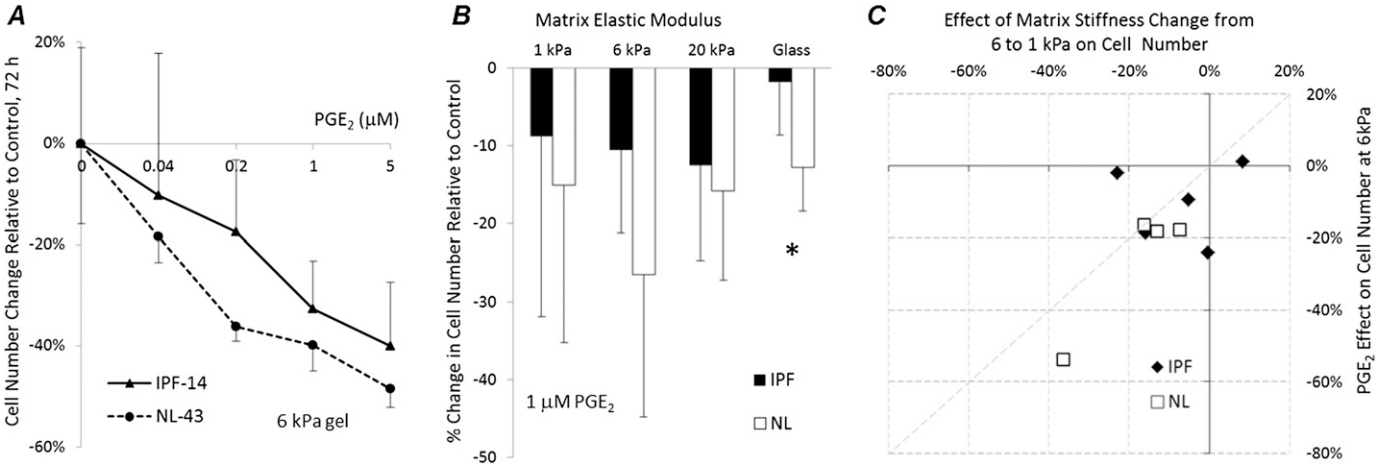

Figure 5. PGE_2 more potently inhibits normal compared with IPF fibroblast proliferation on a rigid matrix. The difference is attenuated on softer matrices. (*A*) Effect of 72-hour PGE_2 dose on change in cell numbers, relative to mean cell number in untreated control samples observed for one fibrotic (IPF-14) and one normal (NL-43) fibroblast line grown on 6-kPa gels. Data represent the mean ± SD of four independent cell counts for each point, relative to the average of four cell counts in untreated control samples. (*B*) Percent change in cell numbers, 72 hours after treatment with 1 μM PGE_2. Data were obtained from three independent cell counts for each of five IPF and four normal fibroblast sources (not shown), and present the average (± SD) change in cell numbers relative to untreated control samples across disease state for each stiffness condition. The *asterisk* marks a statistically significant difference in average cell number change between IPF and normal lung fibroblasts under indicated stiffness conditions (*$P <$ 0.05, two-tailed *t* test). (*C*) Scatterplot compares the effects of 1 μM PGE_2 and changes in substrate stiffness on changes in cell number. Data points indicate average percent changes in cell numbers on 6-kPa gels, 72 hours after treatment with 1 μM PGE_2, relative to untreated control values, versus percent differences between mean cell number changes on 6-kPa and 1-kPa gels for each fibroblast source.

inhibitory effect of PGE_2 on the proliferation of normal but not IPF-derived fibroblasts when cultured on rigid collagen-coated glass (Figure 5B). However, the responses to PGE_2 were not significantly different between the two groups on any of the PA hydrogel matrices (e.g., at 6 kPa, $P = 0.185$, two-tailed *t* test), although PGE_2 did attenuate cell numbers significantly under each condition, except on the softest (1 kPa) matrices (Figure 5B). In contrast to the traction results, the magnitude of the PGE_2 effect on cell number was highly comparable to the differences in cell numbers attributable to matrix stiffness (1-kPa versus 6-kPa gels), suggesting comparable sensitivities of IPF and normal tissue–derived fibroblasts to changes in matrix stiffness and PGE_2 treatment for this phenotypic outcome (Figure 5C).

ROCK Inhibition Attenuates Tractions Effectively in Both IPF and Normal Lung Tissue–Derived Fibroblasts

Rho kinase activity is known to increase with matrix stiffness (21), and Y-27632, an inhibitor of ROCK1 and ROCK2, is known to suppress myofibroblast contraction (28). A detailed kinetic study of one IPF-derived and one normal tissue–derived fibroblast line revealed comparable effects of 10 μM Y-27632 on tractions in cells grown on 6-kPa gels (Figure 6A). Immunofluorescent staining for the phosphorylated myosin regulatory light chain, a downstream target of ROCK that controls actomyosin contractile function, confirmed the potent inhibition of ROCK activity in both IPF-derived and normal lung fibroblasts (Figure 6B). Based on these analyses, we compared functional responses to Y-27632 across a representative subset of IPF and normal tissue–derived fibroblasts. We found that ROCK inhibition significantly reduced tractions in all fibroblast lines tested (Figure 6C), and in contrast to the PGE_2 response, we did not observe any differences in responsiveness of IPF and normal fibroblast groups to Y-27632 (Figures 6D and 6E). Treatment for 72 hours with 10 μM Y-27632 modestly inhibited proliferation in both normal and IPF cells in a fashion comparable to the response to PGE_2 (Figure 6F), but with statistically indistinguishable effects on IPF and normal lung fibroblasts (Figures 6G and 6H). Interestingly, one IPF-derived line (IPF-32) demonstrated no effect of ROCK inhibition on proliferation, although tractions were strongly inhibited by ROCK inhibition in the same IPF-derived line.

DISCUSSION

Recent evidence indicates that the mechanical environment in fibrotic tissue may play an important role in regulating cell function, with increasing matrix stiffness contributing to normal fibroblast activation to a proliferative, contractile, and matrix synthetic state that supports fibrosis in a pathological feedback loop (17, 20, 21). However, IPF-derived fibroblasts have previously been shown to differ in important aspects from normal lung tissue–derived fibroblasts, including their loss of responsiveness to the antifibrotic effects of PGE_2, raising the possibility that IPF-derived fibroblasts, like some cancer cell lines, may have lost their responsiveness to matrix stiffness (29). Our study clearly demonstrates that physiological levels of lung ECM stiffness ($\sim$ 1 kPa elastic modulus) remain an important inhibitor of contractile and proliferative function in primary fibroblasts from fibrotic lungs, and shows that such physiologically soft matrices revert differences in contractility and proliferation observed between normal and IPF-derived fibroblasts on stiffer matrices. Importantly, we show for the first time that even in IPF-derived fibroblasts that have acquired resistance to the antifibrotic effects of PGE_2, cells remain highly responsive to decreases in matrix stiffness toward physiological levels. We also showed that IPF-derived and normal fibroblasts were equally responsive to inhibitions of the stiffness-sensitive Rho kinase pathway, indicating that mechanical cues and mechanically activated signaling pathways may offer unique and potent targets for inactivating IPF fibroblasts, even when resistance to other antifibrotic agents is present.

Whereas reductions in matrix stiffness to physiological levels potently inhibited proliferative and contractile responses of both IPF and normal lung tissue–derived fibroblasts, they exerted

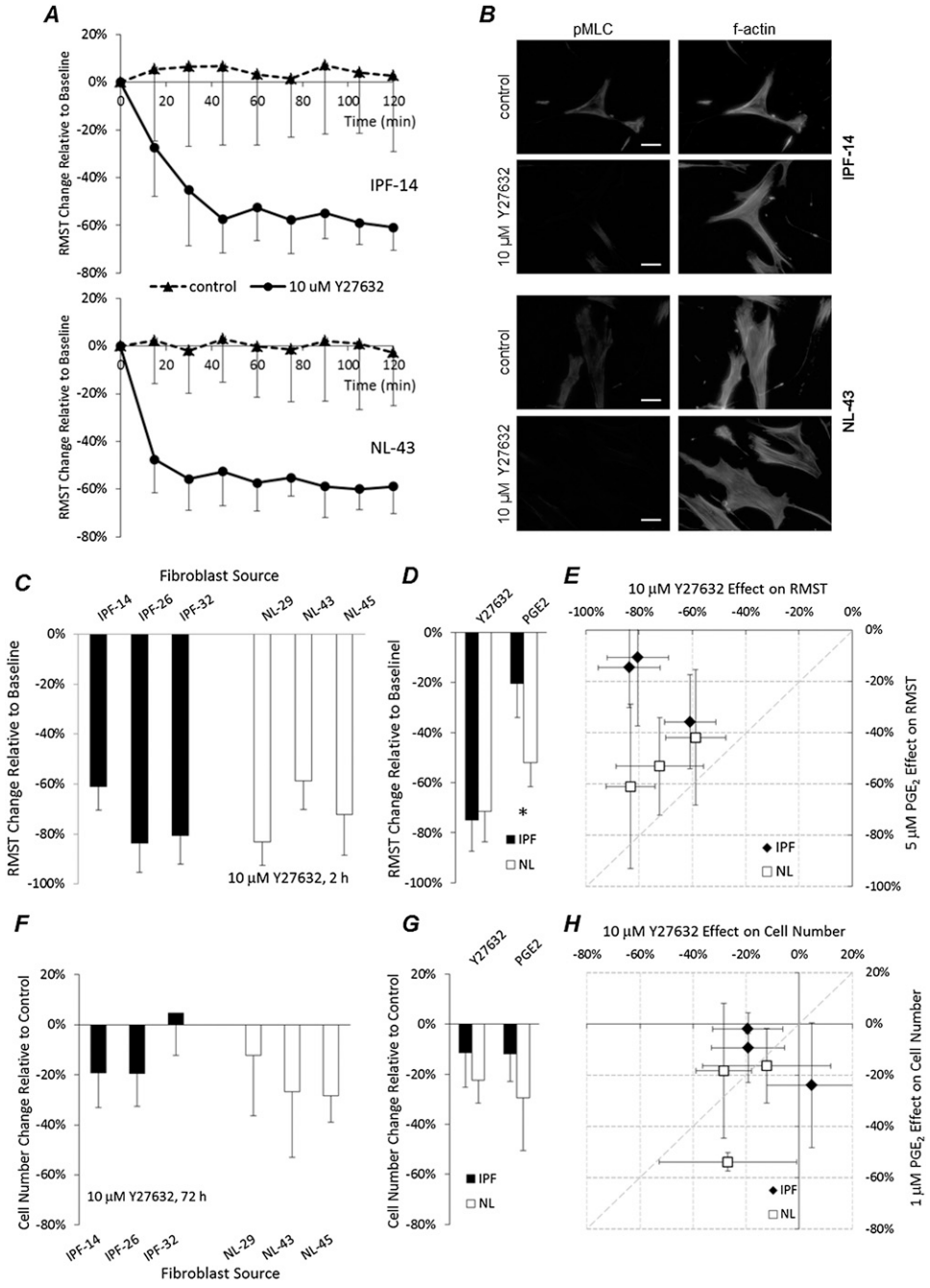

Figure 6. Rho kinase inhibitor robustly diminishes IPF and normal fibroblast tractions. (*A*) Average RMST change time course was measured after the addition of 10 μM Y-27632 (*solid line*) or without treatment (*dashed line*), relative to time zero baseline, in one IPF (*top*) and one normal (*bottom*) fibroblast line grown on PA gels with elastic moduli of 6 kPa. For each time point, data represent the mean (± SD) RMST change measured in 20 cells. (*B*) Immunofluorescence staining of phosphorylated myosin light chain (pMLC; *left column*) in representative IPF (*top two rows*) and normal (*bottom two rows*) fibroblasts cultured for 24 hours on 6-kPa PA substrates, and then treated for 2 hours with or without 10 μM Y-27632. F-actin (*right column*) was labeled with Alexa Fluor–conjugated phalloidin. *Scale bars* = 50 μm. (*C*) RMST change relative to time zero baseline was measured 2 hours after 10 μM Y-27632 treatment. Data represent the mean ± SD from 20 cells for each fibroblast source seeded on 6-kPa PA gels. (*D*) Effects of 10 μM Y-27632 and 5 μM PGE_2 for 2 hours on RMST changes in 6-kPa gels, measured in the subset of IPF and normal lung fibroblast lines presented in *B*. Data represent the mean ± SD within disease conditions. The *asterisk* indicates a statistically significant difference in RMST change between IPF and normal lung fibroblasts (*$P < 0.05$, two-tailed *t* test). (*E*) Scatterplot compares the effects of 10 μM Y-27632 and 5 μM PGE_2 on 2-hour RMST change in 6-kPa gels. Data represent the mean ± SD from 20 (Y-27632) or 15 (PGE_2) cells. (*F*) Cell numbers were assessed 72 hours after the addition of 10 μM Y-27632, relative to average cell numbers of untreated cells. Data represent the mean ± SD of four independent measurements on 6-kPa gel substrates for each fibroblast source. (*G*) Effects of 10 μM Y-27632 and 1 μM PGE_2 for 72 hours on cell numbers in 6-kPa gels, assessed in the subset of IPF and normal lung fibroblast lines presented in *E*. Data represent the mean ± SD within disease conditions. (*H*) Scatterplot compares the effects of 10 μM Y-27632 and 1 μM PGE_2 on cell accumulations, relative to accumulations in untreated control samples, 72 hours after seeding cells. Data represent the mean ± SD from four (Y-27632) or three (PGE_2) independent measurements.

a more modest effect on PGE_2 production, and failed to normalize the differences between IPF and normal fibroblasts. Previous work has shown that low PGE_2 production in IPF fibroblasts results from the reduced expression of COX-2 (14, 17, 30). Recently, impaired COX-2 expression in IPF fibroblasts was linked with an epigenetic mechanism through histone hypoacetylation in the COX-2 promoter region (31). Despite this potential epigenetic regulation of differences between IPF and normal lung–tissue derived PGE_2 production, we note that variations in matrix stiffness retained the capacity to alter PGE_2 concentrations in both groups, and did so with approximately equal potency (although from different baselines), consistent with previous evidence that matrix stiffness regulates COX-2 expression levels (17). Although recent work by Balestrini and colleagues demonstrated that contact with stiff mechanical environments can lead to long-term mechanical memory in fibroblasts (32), out study indicates that in addition to such persistent effects, IPF-derived cells remain acutely responsive to physiologic reductions in matrix stiffness.

Although a comprehensive body of evidence has accumulated documenting the antifibrotic effects of PGE_2 *in vitro* and protection against fibrogenesis in experimental model systems (30, 33–38), IPF fibroblasts were shown to be resistant to the antifibrotic effects of PGE_2 (16). Our results here support these observations, and extend them by showing an impaired ability of PGE_2 to reduce tractions in IPF fibroblasts. One possible explanation for this impaired response may involve the lower production of endogenous PGE_2 in IPF fibroblasts already

discussed. However, the concentrations of PGE_2 produced spontaneously in normal and IPF fibroblasts were in the nanomolar range, whereas the concentrations needed to reduce tractions maximally were in the micromolar range, making this explanation unlikely. Alternatively, previous work indicated that IPF fibroblasts demonstrate highly variable reductions in their expression of the EP2 receptor (16), a G-protein–coupled receptor that signals through the $G\alpha_S$ pathway to mediate the antifibrotic effects of PGE_2. These reductions in EP2 expression arise in part through the hypermethylation of PTGER2, the gene that encodes EP2 expression (27). Here, we observed that transcript levels for PTGER2 were highly variable in IPF fibroblasts relative to normal fibroblast lines, and two out of the three IPF lines examined exhibited substantially diminished PTGER2 transcript levels. However, no systematic relationship was evident between PTGER2 expression and functional responses to PGE_2 in IPF fibroblasts. This is consistent with previous observations that PGE_2 resistance in IPF fibroblasts may also arise because of alterations in the cellular processes occurring downstream of prostanoid receptors, such as the reduced expression of protein kinase A and diminished generation of cyclic adenosine monophosphate in response to receptor activation (16).

Based on the relative resistance of IPF fibroblasts to PGE_2, combined with their retained responsiveness to matrix stiffness, we reasoned that targeting a stiffness-sensitive pathway might offer an attractive alternative for inactivating IPF-derived fibroblasts. ROCK activity is known to scale with matrix stiffness (21), and the contraction of myofibroblasts is dependent on Rho/ROCK/myosin light chain pathway activation (28). Moreover, the ROCK inhibitor Y-27632 was previously shown to attenuate bleomycin-induced lung fibrosis (39), and to promote increased COX-2 expression in normal lung fibroblasts, while inhibiting the formation of α-SMA–positive stress fibers and focal adhesions (17). Our results demonstrate that unlike PGE_2, Y-27632 is equally potent at reducing tractions in both IPF and normal tissue–derived fibroblasts. We note that our traction experiments were performed in the presence of serum (10% FBS) and only 24 hours after seeding, and these conditions are not optimal for α-SMA assembly into actin stress fibers, a prototypical indicator of myofibroblast differentiation. Future work will be needed to examine whether matrix stiffness and the responses of PGE_2 and Y-27632 are maintained under such culture conditions. Rather than acting through alterations in α-SMA, our immunofluorescence imaging indicates that ROCK inhibition attenuated myosin light chain phosphorylation to reduce fibroblast tractions. Intriguingly, the effects of ROCK inhibition on IPF fibroblast proliferation were more modest, and one IPF-derived line exhibited no inhibition of proliferation, even though its traction was highly responsive to Y-27632. These results, although limited to a relatively small set of IPF and normal tissue–derived lung fibroblasts, demonstrate that the contractile and proliferative responses of fibroblasts to ROCK inhibition can be relatively independent, and raise the possibility that some IPF fibroblast functions may exhibit variable responsiveness to ROCK inhibition, an important consideration for therapeutic targeting of this pathway.

In conclusion, our study demonstrates that matrix stiffness within a pathophysiological range controls the contractile and proliferative functions of both IPF and normal lung fibroblasts. Importantly, matrices with normal lung-tissue compliance normalize the differences observed in stiffer matrices, implicating matrix stiffness as an important contributor to fibroblast activation in IPF. Moreover, our results show for the first time that IPF fibroblasts with reduced responsiveness to the antifibrotic mediator PGE_2 remain highly responsive to matrix stiffness and the inhibition of the stiffness-sensitive Rho kinase pathway, indicating that a better understanding of how mechanical cues control fibroblast function may offer new opportunities for targeting these cells, even when they are resistant to antifibrotic pharmacological agents or biological mediators.

Author disclosures are available with the text of this article at www.atsjournals.org.

Acknowledgments: The authors thank Dr. Carol Feghali-Bostwick (University of Pittsburgh, Pittsburgh, PA) who kindly provided the cells for this study, and Dr. Andrew M. Tager (Massachusetts General Hospital, Boston, MA) for helpful discussions.

References

1. Raghu G, Collard HR, Egan JJ, Martinez FJ, Behr J, Brown KK, Colby TV, Cordier J-F, Flaherty KR, Lasky JA, *et al*. An official ATS/ERS/JRS/ALAT statement: idiopathic pulmonary fibrosis: evidence-based guidelines for diagnosis and management. *Am J Respir Crit Care Med* 2011;183:788–824.
2. Katzenstein AL, Myers JL. Idiopathic pulmonary fibrosis: clinical relevance of pathologic classification. *Am J Respir Crit Care Med* 1998; 157:1301–1315.
3. American Thoracic Society and European Respiratory Society. Idiopathic pulmonary fibrosis: Diagnosis and treatment. International consensus statement. *Am J Respir Crit Care Med* 2000;161:646–664.
4. Hinz B, Phan SH, Thannickal VJ, Galli A, Bochaton-Piallat ML, Gabbiani G. The myofibroblast: one function, multiple origins. *Am J Pathol* 2007;170:1807–1816.
5. Hinz B, Phan SH, Thannickal VJ, Prunotto M, Desmouliere A, Varga J, De Wever O, Mareel M, Gabbiani G. Recent developments in myofibroblast biology: paradigms for connective tissue remodeling. *Am J Pathol* 2012;180:1340–1355.
6. Miki H, Mio T, Nagai S, Hoshino Y, Nagao T, Kitaichi M, Izumi T. Fibroblast contractility: usual interstitial pneumonia and nonspecific interstitial pneumonia. *Am J Respir Crit Care Med* 2000;162:2259–2264.
7. Moodley YP, Caterina P, Scaffidi AK, Misso NL, Papadimitriou JM, McAnulty RJ, Laurent GJ, Thompson PJ, Knight DA. Comparison of the morphological and biochemical changes in normal human lung fibroblasts and fibroblasts derived from lungs of patients with idiopathic pulmonary fibrosis during FASL-induced apoptosis. *J Pathol* 2004;202:486–495.
8. Bocchino M, Agnese S, Fagone E, Svegliati S, Grieco D, Vancheri C, Gabrielli A, Sanduzzi A, Avvedimento EV. Reactive oxygen species are required for maintenance and differentiation of primary lung fibroblasts in idiopathic pulmonary fibrosis. *PLoS ONE* 2010;5: e14003.
9. McDonald JA, Broekelmann TJ, Matheke ML, Crouch E, Koo M, Kuhn C III. A monoclonal antibody to the carboxyterminal domain of procollagen Type I visualizes collagen-synthesizing fibroblasts: detection of an altered fibroblast phenotype in lungs of patients with pulmonary fibrosis. *J Clin Invest* 1986;78:1237–1244.
10. Kuhn C, Boldt J, King TE, Crouch E, Vartio T, McDonald JA. An immunohistochemical study of architectural remodeling and connective tissue synthesis in pulmonary fibrosis. *Am J Respir Crit Care Med* 1989;140:1693–1703.
11. Ramos C, Montano M, Garcia-Alvarez J, Ruiz V, Uhal BD, Selman M, Pardo A. Fibroblasts from idiopathic pulmonary fibrosis and normal lungs differ in growth rate, apoptosis, and tissue inhibitor of metalloproteinases expression. *Am J Respir Cell Mol Biol* 2001;24:591–598.
12. Xia H, Diebold D, Nho R, Perlman D, Kleidon J, Kahm J, Avdulov S, Peterson M, Nerva J, Bitterman P, *et al*. Pathological integrin signaling enhances proliferation of primary lung fibroblasts from patients with idiopathic pulmonary fibrosis. *J Exp Med* 2008;205: 1659–1672.
13. Li Y, Jiang D, Liang J, Meltzer EB, Gray A, Miura R, Wogensen L, Yamaguchi Y, Noble PW. Severe lung fibrosis requires an invasive fibroblast phenotype regulated by hyaluronan and CD44. *J Exp Med* 2011;208:1459–1471.
14. Wilborn J, Crofford LJ, Burdick MD, Kunkel SL, Strieter RM, Peters-Golden M. Cultured lung fibroblasts isolated from patients with

idiopathic pulmonary fibrosis have a diminished capacity to synthesize prostaglandin E2 and to express cyclooxygenase-2. *J Clin Invest* 1995; 95:1861–1868.

15. Vancheri C, Sortino MA, Tomaselli V, Mastruzzo C, Condorelli F, Bellistri G, Pistorio MP, Canonico PL, Crimi N. Different expression of TNF-alpha receptors and prostaglandin E(2) production in normal and fibrotic lung fibroblasts: potential implications for the evolution of the inflammatory process. *Am J Respir Cell Mol Biol* 2000;22:628–634.
16. Huang SK, Wettlaufer SH, Hogaboam CM, Flaherty KR, Martinez FJ, Myers JL, Colby TV, Travis WD, Toews GB, Peters-Golden M. Variable prostaglandin E2 resistance in fibroblasts from patients with usual interstitial pneumonia. *Am J Respir Crit Care Med* 2008;177:66–74.
17. Liu F, Mih JD, Shea BS, Kho AT, Sharif AS, Tager AM, Tschumperlin DJ. Feedback amplification of fibrosis through matrix stiffening and COX-2 suppression. *J Cell Biol* 2010;190:693–706.
18. Paszek MJ, Zahir N, Johnson KR, Lakins JN, Rozenberg GI, Gefen A, Reinhart-King CA, Margulies SS, Dembo M, Boettiger D, *et al*. Tensional homeostasis and the malignant phenotype. *Cancer Cell* 2005;8:241–254.
19. Wipff PJ, Rifkin DB, Meister JJ, Hinz B. Myofibroblast contraction activates latent TGF-beta1 from the extracellular matrix. *J Cell Biol* 2007;179:1311–1323.
20. Marinkovic A, Mih JD, Park JA, Liu F, Tschumperlin DJ. Improved throughput traction microscopy reveals pivotal role for matrix stiffness in fibroblast contractility and TGF-beta responsiveness. *Am J Physiol Lung Cell Mol Physiol* 2012;303:L169–L180.
21. Huang X, Yang N, Fiore VF, Barker TH, Sun Y, Morris SW, Ding Q, Thannickal VJ, Zhou Y. Matrix stiffness–induced myofibroblast differentiation is mediated by intrinsic mechanotransduction. *Am J Respir Cell Mol Biol* 2012;47:340–348.
22. Pilewski JM, Liu L, Henry AC, Knauer AV, Feghali-Bostwick CA. Insulin-like growth factor binding proteins 3 and 5 are overexpressed in idiopathic pulmonary fibrosis and contribute to extracellular matrix deposition. *Am J Pathol* 2005;166:399–407.
23. Mih JD, Sharif AS, Liu F, Marinkovic A, Symer MM, Tschumperlin DJ. A multiwell platform for studying stiffness-dependent cell biology. *PLoS ONE* 2011;6:e19929.
24. Weng S, Fu J. Synergistic regulation of cell function by matrix rigidity and adhesive pattern. *Biomaterials* 2011;32:9584–9593.
25. Mio T, Nagai S, Kitaichi M, Kawatani A, Izumi T. Proliferative characteristics of fibroblast lines derived from open lung biopsy specimens of patients with IPF (UIP). *Chest* 1992;102:832–837.
26. Huang S, Wettlaufer SH, Hogaboam C, Aronoff DM, Peters-Golden M. Prostaglandin E(2) inhibits collagen expression and proliferation in patient-derived normal lung fibroblasts via E prostanoid 2 receptor and cAMP signaling. *Am J Physiol Lung Cell Mol Physiol* 2007;292: L405–L413.
27. Huang SK, Fisher AS, Scruggs AM, White ES, Hogaboam CM, Richardson BC, Peters-Golden M. Hypermethylation of PTGER2 confers prostaglandin E2 resistance in fibrotic fibroblasts from humans and mice. *Am J Pathol* 2010;177:2245–2255.
28. Tomasek JJ, Vaughan MB, Kropp BP, Gabbiani G, Martin MD, Haaksma CJ, Hinz B. Contraction of myofibroblasts in granulation tissue is dependent on Rho/rho kinase/myosin light chain phosphatase activity. *Wound Repair Regeneration* 2006;14:313–320.
29. Tilghman RW, Cowan CR, Mih JD, Koryakina Y, Gioeli D, Slack-Davis JK, Blackman BR, Tschumperlin DJ, Parsons JT. Matrix rigidity regulates cancer cell growth and cellular phenotype. *PLoS ONE* 2010; 5:e12905.
30. Keerthisingam CB, Jenkins RG, Harrison NK, Hernandez-Rodriguez NA, Booth H, Laurent GJ, Hart SL, Foster ML, McAnulty RJ. Cyclooxygenase-2 deficiency results in a loss of the anti-proliferative response to transforming growth factor–beta in human fibrotic lung fibroblasts and promotes bleomycin-induced pulmonary fibrosis in mice. *Am J Pathol* 2001;158:1411–1422.
31. Coward WR, Watts K, Feghali-Bostwick CA, Knox A, Pang L. Defective histone acetylation is responsible for the diminished expression of cyclooxygenase 2 in idiopathic pulmonary fibrosis. *Mol Cell Biol* 2009; 29:4325–4339.
32. Balestrini JL, Chaudhry S, Sarrazy V, Koehler A, Hinz B. The mechanical memory of lung myofibroblasts. *Integr Biol (Camb)* 2012;4: 410–421.
33. Lama V, Moore BB, Christensen P, Toews GB, Peters-Golden M. Prostaglandin E2 synthesis and suppression of fibroblast proliferation by alveolar epithelial cells is cyclooxygenase-2–dependent. *Am J Respir Cell Mol Biol* 2002;27:752–758.
34. Kolodsick JE, Peters-Golden M, Larios J, Toews GB, Thannickal VJ, Moore BB. Prostaglandin E2 inhibits fibroblast to myofibroblast transition via E prostanoid receptor 2 signaling and cyclic adenosine monophosphate elevation. *Am J Respir Cell Mol Biol* 2003;29:537–544.
35. Charbeneau RP, Christensen PJ, Chrisman CJ, Paine R III, Toews GB, Peters-Golden M, Moore BB. Impaired synthesis of prostaglandin E2 by lung fibroblasts and alveolar epithelial cells from GM-CSF$^{-/-}$ mice: implications for fibroproliferation. *Am J Physiol Lung Cell Mol Physiol* 2003;284:L1103–L1111.
36. Thomas PE, Peters-Golden M, White ES, Thannickal VJ, Moore BB. PGE(2) inhibition of TGF-beta1–induced myofibroblast differentiation is Smad-independent but involves cell shape and adhesion-dependent signaling. *Am J Physiol Lung Cell Mol Physiol* 2007;293: L417–L428.
37. Maher TM, Evans IC, Bottoms SE, Mercer PF, Thorley AJ, Nicholson AG, Laurent GJ, Tetley TD, Chambers RC, McAnulty RJ. Diminished prostaglandin E2 contributes to the apoptosis paradox in idiopathic pulmonary fibrosis. *Am J Respir Crit Care Med* 2010;182: 73–82.
38. Walker NM, Badri LN, Wadhwa A, Wettlaufer S, Peters-Golden M, Lama VN. Prostaglandin E2 as an inhibitory modulator of fibrogenesis in human lung allografts. *Am J Respir Crit Care Med* 2012;185: 77–84.
39. Shimizu Y, Dobashi K, Iizuka K, Horie T, Suzuki K, Tukagoshi H, Nakazawa T, Nakazato Y, Mori M. Contribution of small GTPase Rho and its target protein ROCK in a murine model of lung fibrosis. *Am J Respir Crit Care Med* 2001;163:210–217.